Viscosity of a Liquid Crystal near the Nematic–Smectic *A* Phase Transition

Anders Madsen,[1,*] Jens Als-Nielsen,[2] and Gerhard Grübel[1]
[1]*European Synchrotron Radiation Facility, B.P. 220, F-38045 Grenoble, France*
[2]*Niels Bohr Institute, Universitetsparken 5, DK-2100 Copenhagen Ø, Denmark*

(Received 20 September 2002; published 26 February 2003)

We report the results of an x-ray scattering study where both the dynamic and the static properties of a liquid crystal (8OCB) near the nematic–smectic *A* phase transition were probed. The static, time-averaged data show the gradual formation of smectic layers in the nematic phase, and we find that the smectic order correlation length parallel to the molecular axis diverges with the critical exponent $\nu_\parallel = 0.70(4)$ at the transition. The literature value is $\nu_\perp = 0.58$ for the perpendicular direction. By x-ray photon correlation spectroscopy, we find that the viscosity coefficient η_3 shows critical, diverging behavior at the phase transition with a critical exponent $x = 0.95(5)$. This contradicts previous light scattering work ($x = 0.50$), but is in good agreement with the theoretical prediction $x = 3\nu_\parallel - 2\nu_\perp$ by Hossain *et al.* [Phys. Rev. B **19**, 432 (1979)].

DOI: 10.1103/PhysRevLett.90.085701 PACS numbers: 64.70.Md, 61.10.–i, 68.03.Kn

It has been demonstrated recently [1] that capillary wave dynamics on a liquid can be measured by x-ray correlation spectroscopy (XPCS) [2]. In this Letter we show how capillary waves can be used to probe the viscosity of an anisotropic fluid. More specifically we present the results of the first XPCS measurement of a liquid crystal (8OCB) near the nematic(N)–smectic *A* (Sm*A*) phase transition. The N-to-Sm*A* transition of the bi-phenyl compound 8OCB has previously been characterized in great detail in static, time-averaged x-ray scattering experiments [3,4]. Here we take the full advantage of combining time-averaged x-ray scattering and XPCS to access both the static and dynamic information simultaneously. The viscosity extracted from the XPCS measurements is diverging with the critical exponent $x = 0.95(5)$ at the N-Sm*A* transition. This is in striking contrast to previously published light scattering results [5] but in good agreement with theoretical predictions based on mode-mode coupling calculations [6].

Liquid crystals are found in many different phases, and a wealth of experiments has led to a rather complete description of their structural properties and phase behavior [7]. The second order N-to-Sm*A* phase transition has been the subject of continued interest since its analogy with the normal-to-superconductor transition was pointed out by de Gennes [8]. In the nematic phase ($T > T_{NA}$) the molecular axes $\overline{n}$ of the elongated molecules are aligned parallel to each other but their centers-of-mass are distributed randomly. This changes in the Sm*A* phase ($T < T_{NA}$), where the aligned molecules are arranged in layers normal to $\overline{n}$ with liquidlike order within each layer. As the second order transition is approached from above, Sm*A* layered clusters with smectic order correlation lengths of $\xi_\parallel$ and $\xi_\perp$ ($\parallel$ parallel, $\perp$ perpendicular to $\overline{n}$) are formed in the bulk. These clusters have no preferred orientation unless an ordering field, arising from an interface, a free surface, an electric field, or a magnetic field, is applied. At the free surface of 8OCB, smectic surface layers (parallel to the surface) are formed simultaneously with the bulk clusters. The lateral extent of these surface layers is essentially infinite while their penetration depth into the bulk coincides with the bulk correlation length [4]. The formation of the oriented surface layers leads to an alignment of the bulk sample with $\overline{n}$ normal to the surface [4,9]. It was predicted [8] that, in analogy to the normal-to-superconductor transition, the correlation lengths $\xi_\parallel$ and $\xi_\perp$ should diverge at the transition, and $\xi_\parallel \propto t^{-\nu_\parallel}$ and $\xi_\perp \propto t^{-\nu_\perp}$ with critical exponents $\nu_\parallel = \nu_\perp = 2/3$ where t is the reduced temperature $t = (T - T_{NA})/T_{NA}$. In a mean-field approach one expects $\nu_\parallel = \nu_\perp = 1/2$. Neither of these values were found experimentally for any investigated system [10] and only a refined theory including crossover effects [11] led to a good agreement with experimental results, e.g., $\nu_\parallel = 0.71$ and $\nu_\perp = 0.58$ for 8OCB [3,4].

In contrast to simple isotropic fluids, the viscosity of a nematic liquid is anisotropic and can be described by three viscosity coefficients η_1, η_2, and η_3 [5] depending on the relative orientation between the flow velocity $\overline{v}$, $\nabla\overline{v}$, and $\overline{n}$. η_{1-3} are usually defined with the help of five Leslie coefficients [5,12] or expressed in terms of the Harvard coefficients ν_{1-5} [13], and only η_3 is expected to diverge at the N-to-Sm*A* transition [5]. If the molecules are aligned parallel to the surface plane, e.g., by applying an ordering field, the capillary wave dynamics will be governed by η_2 for $\overline{q} \perp \overline{n}$ (case A, Fig. 1), while it is determined by both η_1 and η_3 for $\overline{q} \parallel \overline{n}$ (case B). Capillary wave motion in magnetically aligned liquid crystals has been studied by laser light scattering [5,14] in the vicinity of the N-to-Sm*A* transition. The coefficients η_1 and η_2 were both found to exhibit a nondiverging Arrhenius behavior, whereas η_3 was reported to show critical, diverging behavior. Our viscosity measurement was performed in the free surface geometry, and hence all 8OCB molecules are aligned perpendicular to the surface by the surface field. The capillary wave will

0031-9007/03/90(8)/085701(4)$20.00

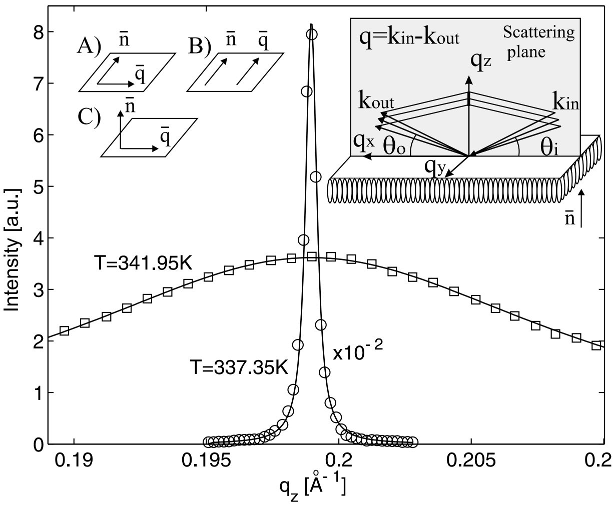

FIG. 1. Specular q_z scans near the smectic layering peak at two different temperatures ($T > T_{NA}$ and $T < T_{NA}$). The peak position corresponds to $\theta_o = \theta_i = 1.40°$. The insets show a sketch of the scattering geometry (right) and illustrate possible orientations $\overline{n}$ of the 8OCB molecules relative to the propagation direction $\overline{q}$ of the capillary waves at the surface (left).

then propagate perpendicular to the molecular axis ($\overline{q} \perp \overline{n}$, case C in Fig. 1) and the dynamics will depend on both η_1 and η_3 [9].

The experiment was carried out at the Troïka beamlines ID10A + B at the European Synchrotron Radiation Facility (ESRF) and x rays with a wavelength of 1.55 Å ($E = 8.02$ keV) were used. The XPCS measurements require a partially coherent beam, implying the beam collimation to match the transverse coherence lengths ($\sim 10\ \mu$m) at the sample position [15]. This was accomplished by selecting the central part of the undulator cone with the help of a pinhole aperture of 10 μm diameter placed upstream of the sample. For the static, time-averaged measurements the beam size was $30(v) \times 1000(h)\ \mu\text{m}^2$. The 8OCB sample (octyloxycyanobiphenyl with a purity better than 99.9%, purchased from SYNTHON AcMaRi, Germany) was kept in an aluminum trough mounted on a heating stage in a closed cell with appropriate temperature control ($\Delta T < 0.02$ K). To minimize parasitic air scattering, the cell was He filled during the experiment. The amount of 8OCB was chosen such that it formed an extended drop (approximately 80 mm wide and 0.5 mm deep) in the isotropic phase ($T > 353$ K). The beam was bent down onto the surface and the incidence angle θ_i was kept constant at 0.1° during the XPCS measurements. During the static, time-averaged scattering experiment the incident and exit angles were simultaneously scanned around 1.40° to record the specular q_z scan (Fig. 1, inset). The scattered intensity was measured by a scintillation detector mounted at the exit of an evacuated flight tube. For the XPCS measurements the detector output signal was processed by an autocorrelator device that computed the time correlation function $g_2(\tau)$ online.

8OCB forms layers in the SmA phase with a d spacing of 31.5 Å and therefore a pronounced peak at $q_0 = 2\pi/31.5\ \text{Å} = 0.199\ \text{Å}^{-1}$ is expected in an x-ray reflectivity scan [4]. This is confirmed in the present experiment. Figure 1 shows two q_z scans around the peak in the nematic phase ($T = 341.95$ K) and in the smectic-A phase ($T = 337.35$ K). The line shape of the peak can be described by

$$S(\mathbf{q}) = \frac{C}{1 + \xi_\parallel^2(q_z - q_0)^2 + \xi_\perp^2 q_\perp^2 + \xi_s^4 q_\perp^4}, \qquad (1)$$

where $C = ct^{-\gamma}$ is the smectic susceptibility and $q_\perp$ is the component of the momentum transfer in the plane of the surface ($q_\perp = \sqrt{q_x^2 + q_y^2}$). The quartic term in Eq. (1) has its origin in layer fluctuations that depend on the elastic constants of the smectic, and ξ_s is the splay correlation length [4]. The solid lines in Fig. 1 show fits to the data using Eq. (1) convoluted with a box function to account for the instrumental resolution in q space. In addition, a constant background was subtracted. The extracted correlation lengths $\xi_\parallel$ (parallel to $\overline{n}$) are plotted in Fig. 2 as a function of the reduced temperature t. $\xi_\parallel$ shows critical behavior, and a power-law fit to the data yields the exponent $\nu_\parallel = 0.70(4)$ in good agreement with previously published results ($\nu_\parallel = 0.71$ [3]). The inset of Fig. 2 shows the smectic susceptibility C derived from the fits as a function of reduced temperature t. The data follow a power law with the exponent $\gamma = 1.31(4)$ in good agreement with literature values [3,4].

The viscosity of 8OCB was measured by XPCS [1,2]. The incidence angle θ_i of the coherent x-ray beam was

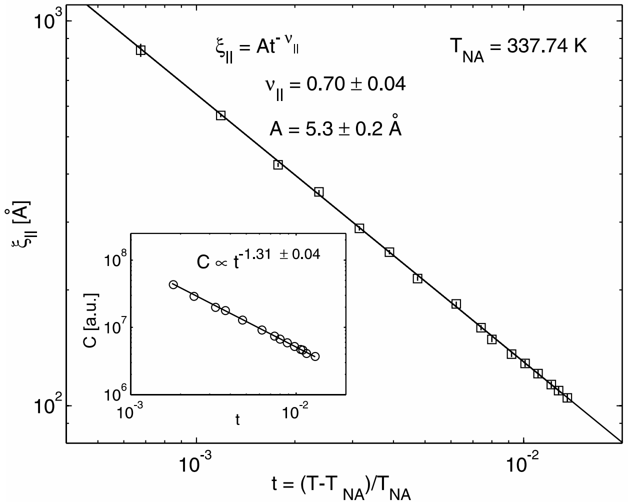

FIG. 2. Critical behavior of $\xi_\parallel$ as a function of t. The solid line is a power-law fit with the parameters given in the figure and $T_{NA} = 337.74$ K. The inset shows the critical behavior of the smectic susceptibility C (arbitrary units).

kept below the critical angle for total external reflection. The take-off angle θ_o of the scattered beam was varied by translating the detector and thereby varying $q_x = 2\pi(\cos\theta_i - \cos\theta_o)/\lambda$ with q_x being the momentum transfer in the scattering plane, parallel to the surface. Time correlation functions $g_2(q, \tau) = \langle I(q, t)I(q, t + \tau)\rangle/\langle I\rangle^2$ were recorded for different momentum transfers q_x and for different temperatures. Here $I(q, t)$ is the scattered intensity, and the brackets denote the time average. The relaxation rate τ_0^{-1} was determined by fitting a single exponential $g_0 e^{-\tau/\tau_0} + 1$ to the measured homodyne correlation function $g_2(\tau)$. Figure 3 shows the relaxation rates τ_0^{-1} as a function of q_x for $T = 338.65$ K. All measured correlation functions were well described by a simple exponential form (inset of Fig. 3), and thus we exclude the existence of any other dynamic processes in the experimentally accessible time window ($1\ \mu\text{sec} \lesssim \tau_0 \lesssim 50$ sec). The dispersion relation for capillary waves [16] predicts overdamped modes ($\tau_o^{-1} \propto q_x$) to decorate high viscosity liquids, while propagating modes ($\tau_o^{-1} \propto q_x^2$) are expected on low viscosity surfaces. The data in Fig. 3 unambiguously show a linear relationship between the relaxation rate τ_0^{-1} and q_x proving that the surface dynamics is dominated by overdamped modes. In the overdamped regime, $\tau_0^{-1} = q_x\sigma/\eta$, where η is the viscosity and σ the surface tension. The solid line in Fig. 3 is the result of a linear least squares fit to the data yielding $\sigma/\eta = 35.76(84)$ cm/sec at $T = 338.65$ K. Overdamped dynamics was found for all investigated temperatures ($337 \lesssim T \lesssim 348$ K). Since the surface tension ($\sigma = 28$ dyn/cm [5,14]) is largely unaffected by the phase transition, the data reflect the temperature dependence of the viscosity. The temperature dependence of η is shown in Fig. 4 (open circles) indicating a diverging behavior at the phase transition (dashed line).

Since the director $\overline{n}$ in the bulk liquid is aligned by the smectic A surface layers [4,9], the capillary waves are propagating normal to $\overline{n}$, and the viscosity η for a completely aligned sample is given by [5]

$$\eta = \eta_1\sqrt{1 + \eta_3/4\eta_1}. \tag{2}$$

The viscosity coefficient η_1 is nondiverging at the transition and follows a simple Arrhenius behavior. Using literature values [5] for η_1 (see Fig. 4) one can extract η_3 with the help of Eq. (2) from the experimental data. The result is shown in Fig. 4 (open squares). The data can be modeled by

$$\eta_3 = At^{-x} + B, \tag{3}$$

where A is a constant, t is the reduced temperature, x is the critical exponent, and B is a nondiverging contribution to η_3 [17]. The determination of the exponent x is very sensitive to a correct evaluation of the transition temperature T_{NA}, and we used the result ($T_{NA} = 337.74$ K) of the least squares fit to the static x-ray scattering data (Fig. 2) thus reducing the number of free parameters when fitting Eq. (3) to the viscosity data. The result of the fit is shown by the solid line in Fig. 4 and yields $x = 0.95(5)$. This is in striking contrast to the mean-field exponent $x = 1/2$ reported in previous light scattering work [5]. The observed exponent is, however,

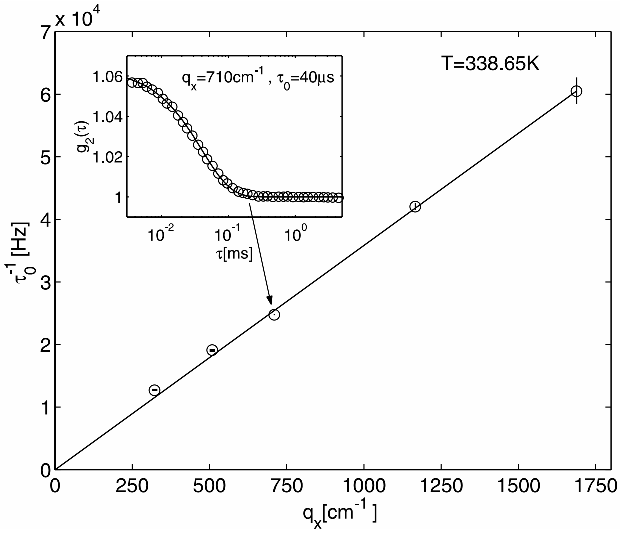

FIG. 3. Variation of relaxation rate as a function of in-plane wave-vector q_x at $T = 338.65$ K. The solid line is a linear fit with slope 35.76 ± 0.843 cm/sec. The inset shows an intensity autocorrelation function $g_2(\tau)$ taken at $q_x = 710\ \text{cm}^{-1}$ described by a single exponential decay. The amplitude (contrast) depends on the experimental setup and was kept constant at ~1.06.

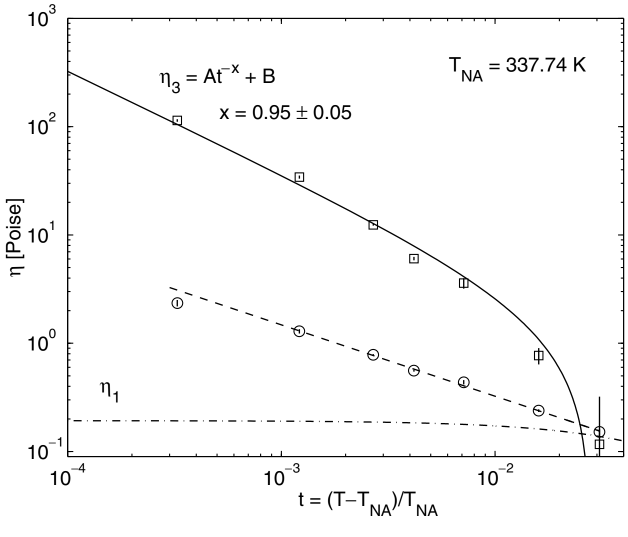

FIG. 4. η (open circles) vs reduced temperature t. The dashed line is a guide to the eye indicating the diverging nature of the data. η_3 (open squares) was determined from η with the help of Eq. (2) and η_1 (dash-dotted line) from Ref. [5]. The solid line is a fit of Eq. (3) to the η_3 data yielding $x = 0.95(5)$, $A = (5.8 \pm 1.6) \times 10^{-2}$ poise, and $B = -1.5 \pm 1.2$ poise.

in good agreement with a theoretical prediction by Hossain, Swift, Chen, and Lubensky [6]. Using the Harvard notation for the viscosity coefficients, η_3 can be expressed in terms of the coefficients ν_{1-3} [13] and

$$\eta_3 = 2(\nu_1 + \nu_2 - 2\nu_3). \tag{4}$$

It was shown [6] that only ν_1 diverges at the N-to-Sm*A* transition while $\nu_{2,3}$ were predicted to exhibit a nondiverging behavior, thus substantiating the parametric form of Eq. (3). Because $\nu_1 \propto \xi_\parallel^3/\xi_\perp^2$ is determined by the static correlation lengths [6] one finds, using Eq. (4), that

$$x = 3\nu_\parallel - 2\nu_\perp. \tag{5}$$

By inserting $\nu_\perp = 0.58$ and $\nu_\parallel = 0.70$ (from Fig. 2) we obtain $x = 0.94$ in good agreement with our least squares fit result 0.95(5) (Fig. 4).

We presently do not have a definitive explanation for the different exponent found in the former light scattering work. However, we note that we are able to independently determine the transition temperature T_{NA} by static x-ray scattering (Fig. 2). This facilitates a precise determination of the exponent from the dynamic data (Fig. 4), which is not possible by light scattering techniques due to the limited accessible q range. In this context it is noteworthy that conflicting exponents ($x = 0.52$ [5] and $x = 0.83$ [14]) have also been published for another liquid crystal compound, CBOOA [5,14]. Using the static exponents for CBOOA $\nu_\parallel = 0.70$ and $\nu_\perp = 0.62$ [3] as input for Eq. (5), one finds $x = 0.86$ which is in good agreement with the viscosity measurement ($x = 0.83$) of Ref. [14].

We acknowledge the assistance of B. Struth during parts of the experiment and thank D. Langevin (Laboratoire de Physique des Solides, Université Paris-Sud), A. Muratov and E. Kats (Institute Laue-Langevin, Grenoble), as well as W. H. de Jeu (FOM-Institute AMOLF, Amsterdam) for helpful conversations.

---

*Electronic address: amadsen@esrf.fr

[1] T. Seydel, A. Madsen, M. Tolan, G. Grübel, and W. Press, Phys. Rev. B **63**, 073409 (2001).

[2] S. Brauer *et al.*, Phys. Rev. Lett. **74**, 2010 (1995); T. Thurn-Albrecht *et al.*, Phys. Rev. Lett. **77**, 5437 (1996); O. K. C. Tsui and S. G. J. Mochrie, Phys. Rev. E **57**, 2030 (1998); A. Malik *et al.*, Phys. Rev. Lett. **81**, 5832 (1998); G. Grübel *et al.*, J. Appl. Crystallogr. **33**, 424 (2000); J. Lal *et al.*, Eur. Phys. J. E **4**, 263 (2001); I. Sikharulidze *et al.*, Phys. Rev. Lett. **88**, 115503 (2002).

[3] J. D. Litster *et al.*, J. Phys. (Paris), Colloq. **40**, C3-339 (1979).

[4] J. Als-Nielsen *et al.*, Phys. Rev. Lett. **48**, 1107 (1982); P. S. Pershan and J. Als-Nielsen, Phys. Rev. Lett. **52**, 759 (1984); K. K. Chan *et al.*, Phys. Rev. Lett. **54**, 920 (1985); P. S. Pershan *et al.*, Phys. Rev. A **35**, 4800 (1987); W. G. Bouwman and W. H. de Jeu, Phys. Rev. Lett. **68**, 800 (1992).

[5] D. Langevin and M. A. Bouchiat, J. Phys. (Paris), Colloq. **33**, C1-77 (1972); D. Langevin, J. Phys. (Paris) **37**, 901 (1975); *Light Scattering by Liquid Surfaces and Complementary Techniques*, edited by D. Langevin (Marcel Dekker, New York, 1992).

[6] K. A. Hossain, J. Swift, J.-H. Chen, and T. C. Lubensky, Phys. Rev. B **19**, 432 (1979).

[7] P. S. Pershan, *Structure of Liquid Crystal Phases* (World Scientific, Singapore, 1988).

[8] P. G. de Gennes, Solid State Commun. **10**, 753 (1972); Mol. Cryst. Liq. Cryst. **21**, 49 (1973); P. G. de Gennes and J. Prost, *The Physics of Liquid Crystals* (Oxford Science Publishing, Oxford, 1993)

[9] A. Madsen, B. Struth, and G. Grübel (to be published).

[10] G. Nounesis *et al.*, Phys. Rev. E **47**, 1910 (1993); C.W. Garland *et al.*, Phys. Rev. E **47**, 1918 (1993); **49**, 2964 (1994).

[11] B. R. Patton and B. S. Andereck, Phys. Rev. Lett. **69**, 1556 (1992); B. S. Andereck and B. R. Patton, Phys. Rev. E **49**, 1393 (1994).

[12] F. M. Leslie, Q. J. Mech. Appl. Math. **19**, 356 (1966); O. Parodi, J. Phys. (Paris) **31**, 581 (1970).

[13] P. C. Martin, P. S. Pershan, and J. Swift, Phys. Rev. Lett. **25**, 844 (1970); D. Forster, T. Lubensky, P. C. Martin, J. Swift, and P. S. Pershan, Phys. Rev. Lett. **26**, 1016 (1971).

[14] C. H. Sohl, K. Miyano, J. B. Ketterson, and G. Wong, Phys. Rev. A **22**, 1256 (1980).

[15] G. Grübel and D. L. Abernathy, Proc. SPIE-Int. Soc. Opt. Eng. **3154**, 103 (1997).

[16] V. G. Levich, *Physicochemical Hydrodynamics* (Prentice-Hall, Englewood Cliffs, NJ, 1962).

[17] B is expected to show an Arrhenius-type behavior $\sim e^{\varepsilon/kT}$ with an activation energy ε. Its temperature dependence is, however, estimated to be small in the relevant temperature range for 8OCB [5], and B is therefore taken to be a temperature independent fit parameter. In other cases this approximation might not apply; cf. A. F. Martins, A. C. Diogo, and N. P. Vaz, Ann. Phys. (Paris) **3**, 361 (1978).